# Direct and Inverse Micelles of Diblock Copolymers with a Polyelectrolyte Block: Effect of Equilibrium Distribution of Counterions

**ARTICLE** *in* MACROMOLECULES · DECEMBER 2010

Impact Factor: 5.8 · DOI: 10.1021/ma102264g



**3 AUTHORS**, INCLUDING:

Sergey V Venev
University of Massachusetts Medical School
**20** PUBLICATIONS **18** CITATIONS
SEE PROFILE

Peter Reineker
Universität Ulm
**299** PUBLICATIONS **3,872** CITATIONS
SEE PROFILE

Macromolecules
ARTICLE

*Macromolecules* **2010**, *43*, 10735–10742 **10735**
DOI: 10.1021/ma102264g

# Direct and Inverse Micelles of Diblock Copolymers with a Polyelectrolyte Block: Effect of Equilibrium Distribution of Counterions

**Sergey V. Venev,[†,‡] Peter Reineker,[§] and Igor I. Potemkin*[,†,‡]**

[†]*Department of Physics, Moscow State University, Moscow 119991, Russian Federation,*
[‡]*Department of Polymer Science, University of Ulm, 89069 Ulm, Germany, and*
[§]*Department of Theoretical Physics, University of Ulm, 89069 Ulm, Germany*

*Received October 1, 2010; Revised Manuscript Received November 7, 2010*

ABSTRACT: We develop a mean-field theory of micelle formation in salt-free solution of diblock copolymers with a soluble polyelectrolyte block and an insoluble neutral block. The so-called *three-zone* model is used which is a simplified alternative of the Poisson−Boltzmann approximation. This model allows to analyze an inhomogeneous distribution of counterions outside the corona (an analogue of Gouy−Chapman layer and Manning condensation). We study both dilute and concentrated solutions. Conventional spherical, cylindrical and planar morphologies of "direct" (soluble) micelles are considered in the crew-cut regime (short soluble blocks). We also analyze the stability of inverse (insoluble) spherical and cylindrical micelles, which form a dense phase. In this phase, the soluble blocks with the solvent form spherical (cylindrical) cores which are embedded in a matrix of the insoluble blocks. Phase diagrams of the solution are constructed on the basis of conditions of the true equilibrium, i.e., they include one- and two-phase stability regions as well as triple points. We demonstrate that the presence of charged groups practically does not change the phase behavior of the solution at high polymer concentrations. In this regime, the main factor governing the swelling of the coronae is the polymer concentration. On the other hand, the role of the charged groups at low polymer concentrations is very important. The Rayleigh instability prevents formation of nonspherical micelles at low polymer concentrations. The charged groups promote stability of the spherical micelles: they remain stable at conditions when the neutral spherical micelles change morphology or precipitate.

## 1. Introduction

Amphiphilic macromolecules attract considerable attention of researchers due to their ability of self-organization.[1,2] For example, diblock copolymers comprising soluble (solvophobic) and insoluble (solvophilic) blocks form micelles in dilute solutions.[3−9] A dense core of the micelles is formed by insoluble blocks, and swollen blocks in the corona provide stability (solubility) of the micelles. The form of the micelles is primarily controlled by the chemical composition of the copolymer. Spherical micelles are stable if the soluble block is long enough.[4,8] Otherwise, cylindrical (worm-like) micelles, vesicles (closed bilayers) and lamellae are formed (the so-called crew-cut regime).[4,8] In contrast to the primary structure of the macromolecules which *predefines* the morphologies, the response of a system on stimuli (temperature, salt and polymer concentration, pH, etc.) allows to *steer* the process of self-organization. Such responsive systems might be of interest for many applications including drug delivery,[10] nanocontainers for chemical and biochemical reactions, stabilization of colloidal particles,[11,12] etc.

The use of amphiphilic polyelectrolytes as stimuli-responsive systems has an advantage in comparison with neutral ones. Polyelectrolytes are known to be water-soluble and contain charged groups and counterions. The presence of the charged groups can provide long-range electrostatic interactions and counterions can be either mobile or bound[13,14] depending on the strength of the electrostatic interactions (i.e., on the dielectric constant of the medium). Thus, the "polyelectrolyteness" can be considered as an additional tool to govern the self-organization. For example, adding a low-molecular-weight salt screens electrostatic interactions, and the degree of dissociation of weak polyelectrolytes depends on the local pH value. To control micelle formation in solutions of diblock copolymers with one neutral (insoluble) and one charged block, efforts of many researchers were directed to the studies of electrostatic and electrolyte effects. Using the scaling approach, Shusharina et al.[15,16] studied the distribution of counterions between the charged corona and the outer region of spherical micelles in a salt-free dilute solution. They predicted conditions under which all counterions leave the charged corona due to entropic reasons (the so-called Pincus regime), if the fraction of charged units and the concentration of the micelles are low enough. Highly charged micelles keep most of the counterions inside the corona to compensate for its electric charge[15,16] (the so-called osmotic regime). An intermediate regime of partial filling of the corona by counterions was analyzed within the two-zone Oosawa model[17] which assumes homogeneous concentrations of counterions within and outside the corona (step-like distribution function of counterions).[15] Morphological transitions between spherical, cylindrical and lamellar structures were analyzed in the regime of low[18] and high[18,19] salt concentration assuming that local neutrality of the system is fulfilled. In particular, sphere-to-cylinder and cylinder-to-lamella transitions were predicted to occur for crew-cut micelles,[19] i.e., for micelles with short enough soluble blocks. Using similar models with local neutrality, pH-triggered morphological transitions of micelles with weakly dissociating polyelectrolyte block were predicted in refs 20 and 21.

Local violation of electric neutrality in polymer systems due to entropy-driven escape of counterions[22−25] can induce long-range electrostatic forces. For example, the competition of the

*To whom correspondence should be addressed. E-mail: igor@polly.phys.msu.ru.



Published on Web 12/03/2010

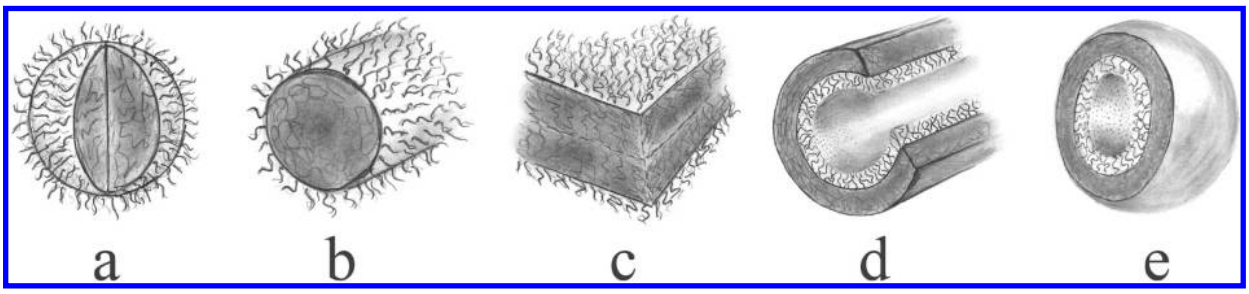


**Figure 1.** Examined structures.

(i) *long-range* electrostatic repulsion of clusters (homogeneous aggregates without core−shell structure) with the (ii) *short-range* attractive forces acting between macromolecules results in the formation of clusters of different morphologies (spheres, cylinders and planar layers) possessing an optimum size.[23,24] In this case, the polymer concentration controls the long-range interactions and the morphology of the aggregates.[23,24] The stabilization of the optimum size of the clusters is related to the classical Rayleigh problem of a charged droplet:[26] a spherical droplet whose charge exceeds some critical value is locally unstable and will spontaneously deform. The equilibrium state of this system is a set of smaller droplets of a certain size with the charge on each of them less than the critical one. However, the charge of the clusters is fully controlled by escaped counterions, i.e., by the average polymer concentration and the stabilization occurs at larger length scales in contrast to the "pure" Rayleigh stabilization in the absence of counterions.[23,24]

Therefore, one can expect that (i) *the local violation of electric neutrality* in micellar solutions together with (ii) the *composition of the block copolymer* are responsible for the size of the micelles and their morphology. To the best of our knowledge, the simultaneous effect of these two factors on the morphology of the micelles in solutions of diblock copolymer with neutral (insoluble) and charged block has not been studied yet.

In the present paper we will develop a theory of micelle formation in salt-free solution. The local violation of electric neutrality (partial escape of counterions from the charged corona of the micelles) will be taken into account within the so-called *three-zone* model. One of the zones corresponds to the corona, and the outer solvent (related to one micelle) is divided into two zones. The position of the boundary between these two zones is determined from the minimization of the free energy. Such a division of the outer solution allows to describe the inhomogeneous distribution of counterions outside the micelles that models counterion condensation[27] (cylindrical micelles) and double layer formation[28,29] (lamellae). Real phase diagrams based on equalities of the osmotic pressures and the chemical potentials of coexisting phases will be constructed. These diagrams include dilute, semidilute, and concentrated regimes.

## 2. Model

Let us consider solution of an AB diblock copolymer with a neutral, insoluble A block and a weakly charged B block. We suppose that both blocks of the copolymer are flexible and consist of identical statistical segments, each of length $a$ and of excluded volume $v \approx a^3$; $N_A$ and $N_B$ are the numbers of the segments. The B block contains $N_B/\sigma$ charged groups, each of the elementary charge $e$. These groups are homogeneously distributed along the block so that $\sigma \gg 1$ is the average number of neutral segments between two adjacent charged groups along the chain, and $1/\sigma \ll 1$ is the average fraction of the charged groups. The charged groups are completely dissociated and counterions, which provide macroscopic electric neutrality of the system, are mobile. We consider a salt-free solution where counterions are the only low-molecular-weight ions of the system. To provide applicability of the mean-field theory, let us assume that the solvent is a Θ-solvent for the neutral spacers (subchains connecting two adjacent charged segments) of the polyelectrolyte block and triple repulsive interactions of the B segments are quantified by the third virial coefficient $C \approx a^6$. The composition of the copolymer $f$ is defined as $f = N_B/N$, $N = N_A + N_B$.

Diblock copolymers self-assemble into micelles of different morphologies in the selective solvent if the polymer concentration $\varphi$ exceeds the critical micelle concentration (cmc). "Direct" micelles consisting of an insoluble core and a swollen corona are formed at relatively low values of $\varphi$. We will analyze the thermodynamic stability of spherical, cylindrical and lamellar structures, Figure 1a−c. "Inverse" micellar structures can be formed at high polymer concentration values and long insoluble block, Figure 1 d,e. In this case, cylindrical and spherical structures containing swollen B blocks and solvent are embedded in a matrix formed by the insoluble blocks. Analysis of all structures will be done in the strong segregation regime[30] and in highly selective solvent, i.e., the core and the shell of the micelles are assumed to have well-defined shapes with narrow interface (A and B blocks are strongly segregated) and insoluble A blocks form dry (solvent-free) domains.

## 3. Direct Structures

The equilibrium structure of the micelle is determined by the balance between (i) unfavorable contacts of the insoluble blocks with the solvent and (ii) the elastic stretching of the blocks in the core and the corona. The latter is strongly coupled with the distribution of counterions: unscreened repulsion of the charged groups makes the corona swollen in the Pincus regime, and counterions localized in the corona swell it as well due to their high osmotic pressure. Quantitatively, the balance is calculated by minimization of the total free energy of the micelle per chain comprising the core−corona surface energy $F_{surf}$, the elastic free energy of the A blocks $F_{core}$ and the free energy of the corona $F_{corona}$:

$$F = F_{core} + F_{surf} + F_{corona} \tag{1}$$

The elastic free energy of the extended core blocks per chain yields[30]

$$F_{core} = b_j \frac{{R_0}^2}{(1-f)Na^2} \tag{2}$$

where $R_0$ is the radius of the core of the micelle (semithickness in the case of lamella) and coefficients

$$b_j = \begin{cases} \pi^2/8, & j = 1 \\ \pi^2/16, & j = 2 \\ 3\pi^2/80, & j = 3 \end{cases} \tag{3}$$

correspond to different structures: lamellar ($j = 1$), cylindrical ($j = 2$), and spherical ($j = 3$). The inequalities $b_1 > b_2 > b_3$ mean that

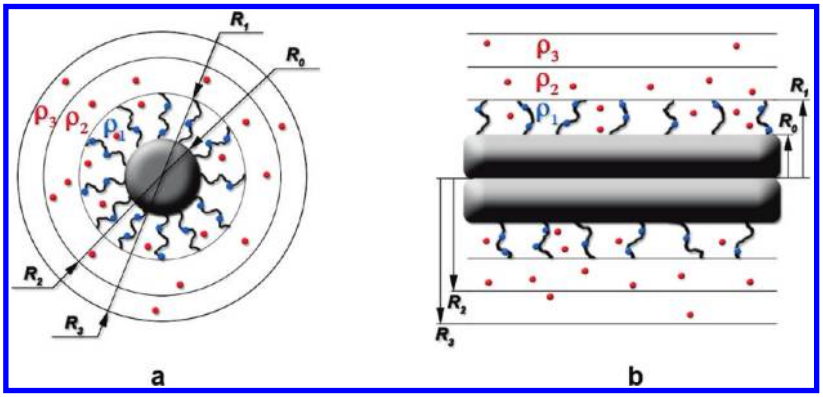


**Figure 2.** Volume per micelle is approximated by a sphere, cylinder (a) or planar layer (b) of the radius (semithickness) $R_3$. The radii of the core and corona are denoted by $R_0$ and $R_1$, respectively. Blue and red dots depict charged groups of the soluble blocks and mobile counteions. The counterions are distributed inhomogeneously. They occupy three zones (excluding the core) denoted by the radii $R_1$, $R_2$, and $R_3$. The boundary between the second and the third zones is determined from equilibrium conditions. $\rho_1$, $\rho_2$, and $\rho_3$ denote different charge densities.

maximum stretching of the A block is achieved in the one-dimensional structure. In contrast, the surface energy of the lamella per chain is minimum:

$$F_{surf} = \gamma \frac{S^{(j)}(R_0)}{Q} = \gamma \frac{j(1-f)Nv}{R_0} \tag{4}$$

Here $S^{(j)}(R_0)$ is the area of the core−corona interface

$$S^{(j)}(R_0) = \begin{cases} 2\Sigma, & j = 1 \\ L2\pi R_0, & j = 2 \\ 4\pi {R_0}^2, & j = 3 \end{cases} \tag{5}$$

and the aggregation number $Q$ is related to the volume of the core $V^{(j)}$ through the dense packing condition:

$$(1-f)NQv = V^{(j)}(R_0) = \begin{cases} 2\Sigma R_0, & j = 1 \\ L\pi {R_0}^2, & j = 2 \\ \frac{4\pi}{3} {R_0}^3, & j = 3 \end{cases} \tag{6}$$

In eq 4, $\gamma$ is the surface tension coefficient related to the thermal energy $k_BT$, so that $\gamma a^2$ is dimensionless parameter. $\Sigma \rightarrow \infty$ and $L \rightarrow \infty$ are the area of the core−corona interface of the lamella and the length of the cylinder, respectively.

Under the strong segregation conditions, the corona can be envisioned as a curved ($j = 2, 3$) or planar ($j = 1$) polyelectrolyte brush. To calculate the free energy of the corona, we employ the mean-field approximation which is justified by consideration of the Θ-solvent regime for the neutral spacers of the swollen blocks. Within this approximation, the corona free energy per chain can be written as follows:

$$F_{corona} = F_{elast} + F_{vir} + F_{el-st} + F_{tr} \tag{7}$$

Here the first term is responsible for the elastic stretching of the blocks:

$$F_{elast} = \frac{3}{2a^2} \int_{R_0}^{R_1} \left(\frac{\mathrm{d}r}{\mathrm{d}n}\right) \mathrm{d}r \tag{8}$$

where $R_1 - R_0$ is the corona thickness. This expression is valid under the assumption that all free ends of the brush are equidistant from the interface (Alexander's approximation[31]). The local stretching of the block $(\mathrm{d}r/\mathrm{d}n)|_r$ at the distance $r$ from the center of the core can be calculated from the space filling condition applied to the thin layer of the thickness $\mathrm{d}r$ which is crossed by $Q$ chains

$$c_p(r) S^{(j)}(r)\, \mathrm{d}r = Q\, \mathrm{d}n, \quad R_0 < r < R_1 \tag{9}$$

where $c_p(r)$ is the concentration of the segments and $dn$ segments of each block belong to the layer. In our further analysis we will be concentrated on morphological transitions in the micellar solution which are known to occur in the crew-cut regime.[4,8] Short soluble blocks provide a weak dependence of the polymer concentration on the coordinate $r$ (spherical and cylindrical shapes), and we assume that $c_p(r)$ has a constant value, $c_p(r) = c_p$:

$$F_{elast} = \frac{3Q}{2a^2 c_p} \int_{R_0}^{R_1} \frac{\mathrm{d}r}{S^{(j)}(r)}$$

$$= \frac{{R_0}^2}{a^2 N} \begin{cases} \dfrac{3f}{2(1-f)^2 c^2}, & j = 1 \\ \dfrac{3}{8(1-f)c} \ln\left(1 + \dfrac{f}{(1-f)c}\right), & j = 2 \\ \dfrac{1}{2(1-f)c}\left(1 - \left(1 + \dfrac{f}{(1-f)c}\right)^{-1/3}\right), & j = 3 \end{cases} \tag{10}$$

where $c = vc_p$, and the space filling conditions for the core, eq 6, and for the corona, $V^{(j)}(R_1) - V^{(j)}(R_0) = fNQ/c_p$, are used.

The second term in eq 7 is the energy of triple collisions of monomer units in a Θ-solvent

$$F_{vir} = c^2 fN \tag{11}$$

which is taken into account within the virial approximation, where the third virial coefficient $C = v^2$.

The average volume of the system related to one micelle can be estimated as the total volume of the system divided by the number of the micelles. Let us approximate this volume by a sphere, cylinder or planar layer of the radius (semithickness) $R_3$ by analogy to the Wigner−Seitz cell of spatially ordered micelles, Figure 2. For the derivation of the electrostatic energy $F_{el-st}$, let us generalize the Oosawa model[17] and consider three zones. The volume accessible for counterions (whole volume excluding the core) is divided into three zones. The concentration of counterions within each zone is assumed to be constant (step-like concentration profile). The first zone with radius $R_1$ corresponds to the corona. The polymer-free region is divided into two zones (2 and 3) and the boundary between these zones with radius $R_2$ is

determined from equilibrium conditions. Let $\beta$ is the fraction of counterions in the first zone, so that their total number in the zone is $\beta QN_B/\sigma$. The rest $(1-\beta)QN_B/\sigma$ counterions are distributed between the second and the third zones: $\lambda(1-\beta)QN_B/\sigma$ counterions occupy the second zone and $(1-\lambda)(1-\beta)QN_B/\sigma$ counterions are localized in the third zone, $0 \le \lambda \le 1$. Using the space-filling conditions for the core and the corona as well as the definition of the average polymer concentration $\varphi$ in the solution, $V^{(j)}(R_3)\varphi = QNv$, we obtain for the concentration of counterions

$$c_c(r) = \begin{cases} c_{c1} = \dfrac{c_p}{\sigma}\beta, & R_0 < r < R_1 \\ c_{c2} = \dfrac{c_p}{\sigma}\dfrac{\lambda(1-\beta)f\varphi}{c(\alpha-(1-f)\varphi)-f\varphi}, & R_1 < r < R_2 \\ c_{c3} = \dfrac{c_p}{\sigma}\dfrac{(1-\lambda)(1-\beta)f\varphi}{c(1-\alpha)}, & R_2 < r < R_3 \end{cases} \tag{12}$$

and for the charge density

$$\rho(r) = \begin{cases} \rho_1 = \dfrac{ec_p(1-\beta)}{\sigma}, & R_0 < r < R_1 \\ \rho_2 = -ec_{c2}, & R_1 < r < R_2 \\ \rho_3 = -ec_{c3}, & R_2 < r < R_3 \end{cases} \tag{13}$$

In eq 12, $\alpha$ is defined as $V^{(j)}(R_2) = \alpha V^{(j)}(R_3)$, $\alpha < 1$.

The electrostatic energy of the charged corona and the outer region can be calculated in a standard way

$$F_{el-st} = \frac{\varepsilon}{8\pi k_B TQ}\int_{V^{(j)}(R_3)-V^{(j)}(R_0)} \mathrm{d}V^{(j)}\, E^2(r) \tag{14}$$

where $E(r)$ is intensity of the electric field at the distance $r$ and $\varepsilon$ is the dielectric constant of the solvent (the polymer volume fraction in the corona is assumed to be small). The intensity is related to the charge density via Gauss's law. For simple morphologies, it takes the form:

$$\oint d\vec{S}^{(j)}\vec{E} = S^{(j)}(r)E(r) = \frac{4\pi}{\varepsilon}\int_{V^{(j)}(r)-V^{(j)}(R_0)} \mathrm{d}V^{(j)}\,\rho(r) \tag{15}$$

For example, from eq 15 $E(r)$ of the spherical micelle is expressed as

$$E(r) = \frac{4\pi}{3r^2}\begin{cases} \rho_1(r^3 - {R_0}^3), & R_0 < r < R_1 \\ \rho_1({R_1}^3 - {R_0}^3) + \rho_2(r^3 - {R_1}^3), & R_1 < r < R_2 \\ -\rho_3({R_3}^3 - r^3), & R_2 < r < R_3 \end{cases} \tag{16}$$

where the condition of the macroscopic electric neutrality

$$\rho_1(V^{(j)}(R_1) - V^{(j)}(R_0)) + \rho_2(V^{(j)}(R_2) - V^{(j)}(R_1)) + \rho_3(V^{(j)}(R_3) - V^{(j)}(R_2)) = 0 \tag{17}$$

is used. The electrostatic energy of all studied morphologies takes the form

$$F_{el-st} = \frac{uN{R_0}^2}{\sigma^2 a^2}A^{(j)}(f, \varphi, c, \alpha, \beta, \lambda) \tag{18}$$

where the function $A^{(j)}$ is different for different morphologies. It has to be noticed that this function depends only on the parameters which are denoted in the brackets. The dimensionless parameter $u$ in eq 18 describes the strength of the electrostatic interactions, $u = e^2/(\varepsilon k_B Ta)$, and $u \approx 1$ in aqueous solutions.

Finally, the last term in the free energy of the corona, eq 7, is the energy of thermal motion of counterions in the zones 1−3:

$$F_{tr} = \frac{1}{Q}\int_{V^{(j)}(R_3)-V^{(j)}(R_0)} \mathrm{d}V^{(j)}\, c_c(r)\ln\{c_c(r)v\} = \frac{\beta fN}{\sigma}\ln(c_{c1}v) + \frac{\lambda(1-\beta)fN}{\sigma}\ln(c_{c2}v) + \frac{(1-\lambda)(1-\beta)fN}{\sigma}\ln(c_{c3}v) \tag{19}$$

The equilibrium free energy of the micelle is calculated via minimization of eq 1 with respect to the parameters $R_0$, $c$, $\alpha$, $\beta$, and $\lambda$. Note that the minimization with respect to $R_0$ can be done analytically and determines the radius (semithickness) of the core of the micelle and the aggregation number using the space-filling condition. The minimization with respect to other parameters is performed numerically. These parameters are responsible for the distribution of the counterions between the zones ($\beta$, $\lambda$), for the swelling of the corona ($c$), and for the location of the boundary between the second and the third zones ($\alpha$).

One important conclusion comes from the form of the elastic free energies of blocks, eqs 2, 10, and of the electrostatic energy $F_{el-st}$, eq 18. All these contributions are positive and proportional to ${R_0}^2$. Therefore, both the elasticity of the blocks and the electrostatic interactions play a stabilizing role preventing the micelles from aggregation (the growth of the micelles in size ($R_0$) increases the corresponding contributions to the free energy). Keeping in mind that $F_{el-st}$ depends on the polymer concentration of the solution (on the distribution of the counterions between the corona and the outer solution), one can expect that the morphology of the micelles is also concentration dependent. This expectation will be demonstrated in the phase diagrams below.

In the case of high polymer concentration, when the micelles are densely packed, the expression for the total free energy has to be modified. First of all, we keep the spherical, cylindrical and planar forms of the micelles (i.e., we neglect the deformation of the coronae under the packing). Also we assume that interpenetration of the coronae is negligible due to the high stretching of the corona-forming blocks (interpenetration would increase the stretching). The average volume per micelle in the solution becomes equal to the volume of the micelle, i.e. the second and third zones disappear and all counterions are localized within the corona making it neutral. Therefore, $\beta = 1$, $F_{el-st} = 0$, and $c$ is no longer a minimization parameter: it is related to the average polymer concentration via

$$c = \frac{f\varphi}{1-\varphi(1-f)} \tag{20}$$

It is clear that within our model the transition into the concentrated mode is "smooth" and, therefore, binodal lines on phase diagrams have also to be smooth.

## 4. Inverse Structures

The crew-cut micelles can be unstable if the length of the soluble (charged) block becomes less than some certain value. In this case, long insoluble blocks can form dense coronae of the micelles and short soluble blocks together with the solvent form loose cores ("lakes" or "channels" with "seaweeds"). Taking into account insolubility of such micelles, one can expect formation of nanostructured precipitant: the "lakes" and the "channels" embedded in a dense polymer matrix. In this paper we will analyze two morphologies of the inverse micelles: spherical and cylindrical, Figure 1d,e. The formation of polymer−solvent interphase

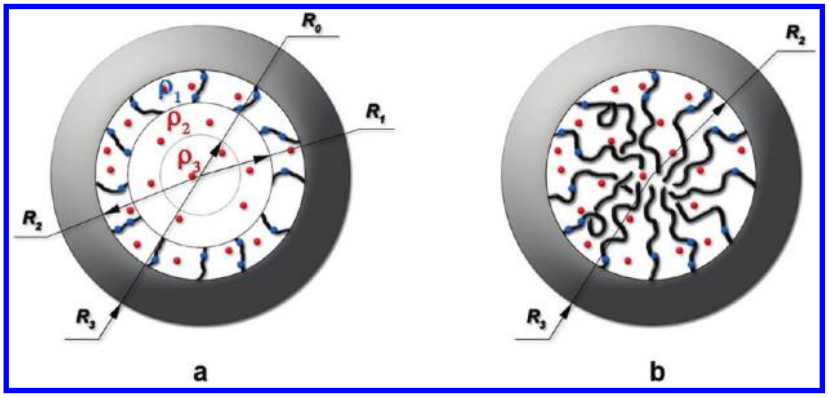


**Figure 3.** Two kinds of the core of the inverse structures: a hollow core with the soluble blocks on the periphery (a), and a filled core (b). The hollow core is locally charged (being totally neutral) and the filled core is locally neutral.

does not cost energy, if the polymer is soluble. Therefore, we can analyze the stability of two structures of the soluble core: the B blocks occupy only periphery forming hollow core, Figure 3a, and they fill in the whole volume of the core more or less homogeneously (filled core), Figure 3b. In the first case, the core is locally charged (being totally neutral) and the filled core is assumed to be locally neutral.

The free energies of the inverse micelles are calculated in a similar way as those in the case of the direct structures. The elastic free energy of the corona is calculated within Alexander's approximation, eq 8, assuming that the polymer volume fraction is equal to unity. The elastic free energies of the hollow core and of the filled core are calculated assuming a constant polymer concentration with equations analogous to eqs 8 and 2, respectively. The volume of the hollow core is also divided into three zones, Figure 3: the electrostatic energy and the entropy of the counterions are calculated like those in eqs 18 and 19. Finally, the electrostatic energy of the filled core equals zero, the counterions are distributed uniformly over the core, and the energy of the excluded volume interactions in the Θ-solvent is calculated by eq 11.

## 5. Phase Diagrams

Phase diagrams of the diblock copolymer in the selective solvent are obtained in a standard way by equating the chemical potentials and the osmotic pressures of coexisting phases. The chemical potential, $\mu$, and the osmotic pressure, $\pi$, of the micellar solution (or inverse micelles) are calculated using the equilibrium free energy of the micelle per chain, $F_{equilib}$, which is the minimum of eq 1 (and analogous expressions for the inverse structures):

$$\mu = \frac{1}{N}\frac{\partial(\varphi F_{equilib})}{\partial\varphi}, \quad \pi = \frac{\varphi^2}{N}\frac{\partial F_{equilib}}{\partial\varphi},$$
$$F_{equilib} = \min_{\{R_0, c, \alpha, \beta, \lambda\}} F \qquad (21)$$

We will fix the parameters $N = 1000$, $u = 1$, $\gamma a^2 = 0.33$ in all our calculations. These values correspond to the aqueous solutions and strongly selective solvent.

A series of phase diagrams in the variables: average polymer volume fraction $\varphi$ and chemical composition of the copolymer (fraction of the soluble B block) $f = N_B/N$ for different values of the fraction of charged units $1/\sigma$ is presented in Figure 4.

Three kinds of direct (soluble) micelles and four kinds of inverse (insoluble) micelles are predicted to be stable in the selective solvent (white areas in the diagram). Stability regions of nonaggregated molecules (below the critical micelle concentration) and homogeneous precipitant (at exponentially small $f$ values) are not depicted in the diagrams because they occupy

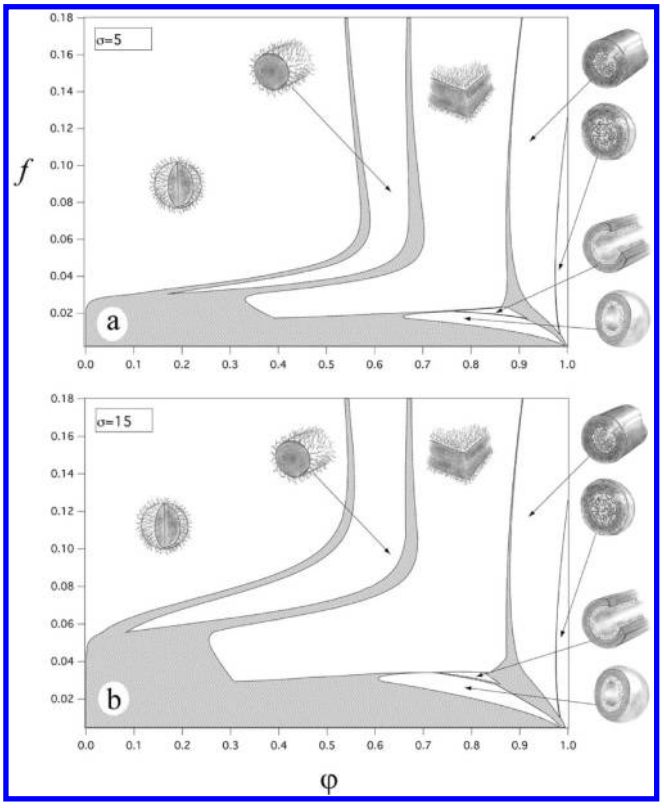


**Figure 4.** $\varphi - f$ phase diagrams of the copolymer for different values of the fraction of charged units $1/\sigma$: $\sigma = 5$ (a), and 15 (b). Shaded area corresponds to the phase coexistence.

vanishingly small areas. Shaded areas correspond to the phase coexistence, and the fractions of the coexisting phases are determined using the Maxwell rule. In contrast to neutral micellar solutions[6] or to theoretical models of charged micelles employing the local electroneutrality condition,[8,9,18−20] the morphologies of the micelles are controlled by the polymer concentration. For example, only the spherical micelles are stable at low polymer concentration whereas cylindrical micelles and lamellae can coexist with the spheres forming dense enough phases (bottom parts of the diagrams in Figure 4). The reason for that is the local violation of electric neutrality of the system. Despite the three-zone model allows condensation of counterions near the cylinders and planar layers, the condensation is incomplete because of the thermal motion of the counterions. Therefore, the electrostatic energy of the cylinders and the planar layers can be decreased only via the decrease of the distance between them. It has to be mentioned that the electrostatic energies of an infinite cylinder

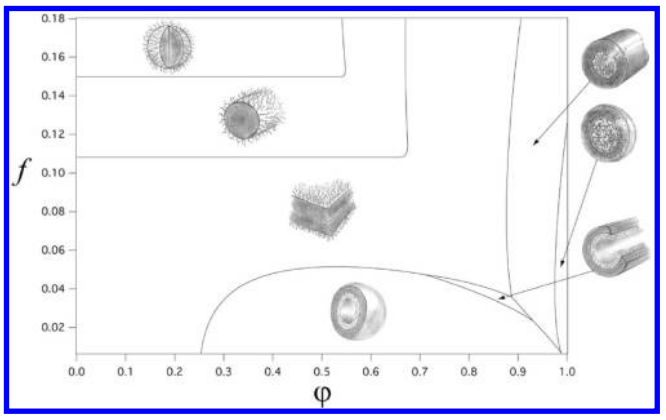


**Figure 5.** Simplified $\varphi-f$ diagram of a neutral copolymer ($\sigma = \infty$) in the selective solvent obtained by equating free energies of different morphologies. $N = 1000$ and $\gamma a^2 = 0.33$.

and a plane logarithmically and linearly increase with the distance from them.[23] Therefore, approaching cylinders or lamellae to each other, i.e. making the phase denser, one can decrease the electrostatic energy. The electrostatic origin of instability of the cylinders and lamellae at small polymer concentrations can be demonstrated also by the shift of the cylinders and lamellae stability regions toward smaller values of $\varphi$ with the decrease of the fraction of charged units (increase of $\sigma$), Figure 4a,b.

As mentioned above, the electrostatic interactions together with elasticity of the blocks play a stabilizing role (both $F_{core}$, $F_{elast}$, and $F_{el-st}$ are positive and proportional to $R_0^2$). This effect can also be extracted from Figure 4. Fixing the polymer concentration and decreasing the composition $f$, one can see that stronger charged spherical micelles ($\sigma = 5$) become unstable at lower value of $f$ than less charged ones ($\sigma = 15$).

Transitions *spheres* → *cylinders* → *lamellae* → *inverse cylinders* → *inverse spheres* with the increase of $\varphi$ in the upper part of the diagram are induced by steric interactions between the micelles. When the coronae of the micelles are in contact with each other, their swelling is determined by the average polymer concentration, eq 20: the higher the concentration, the denser the coronae. In other words, increasing the concentration of the system makes the corona-forming blocks less stretched which leads to the cascade of the transitions.

Inverse spherical micelles with hollow core can coexist with the direct spherical micelles at low polymer concentration. Also this phase can coexist with inverse cylindrical and spherical structures having filled core at high polymer concentration. In has to be noticed that the inverse structures with the filled core have larger area in the $\varphi - f$ phase diagram than those with the hollow core.

Making the soluble block neutral, one can achieve stability of both cylinders and lamellae (which will be transformed into vesicles) at low polymer concentration. A simplified diagram of a neutral copolymer ($\sigma = \infty$) in a selective solvent (poor solvent for one block and Θ-solvent for another block), based on equalities of the free energies, is presented in Figure 5.

Despite the simplified method of construction of this diagram, two main conclusions can be drawn from the comparison with the diagrams of charged copolymers. First, the presence of charged groups practically does not change the phase behavior of the solution at high concentration. Here, the main factor governing the swelling of the coronae is the polymer concentration. Second, (i) the Rayleigh instability,[26] preventing the formation of nonspherical micelles at low polymer concentration, and (ii) the enhancement of the stability of the spherical micelles (a shift of the boundary toward smaller $f$ values) at low $\varphi$ are clearly detectable upon charging the copolymer.

The diagram for the neutral copolymer has a qualitative correlation to the experimental one obtained for PEO−PB di-

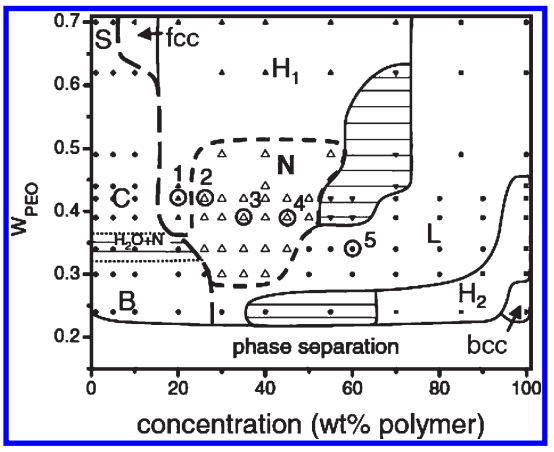


**Figure 6.** Phase portrait for the PEO−PB diblock copolymers in water as a function of composition ($W_{PEO}$) and the concentration of copolymer in solution.[32] Solid lines mark the morphology boundaries and thin horizontal lines identify regions of morphology coexistence. Spherical (S) and cylindrical (C) micelles, and vesicles (B), were characterized at low concentration by cryo-TEM. Cubic (fcc and bcc), hexagonal (H1 and H2), lamellar (L), and network (N) morphologies were identified based on SAXS and cryo-SEM. Reprinted with permission from Jain, S.; Gong, X.; Scriven, L. E.; Bates, F. S. *Phys. Rev. Lett.* **2006**, *96*, 138304. http://dx.doi.org/10.1103/PhysRevLett.96.138304. Copyright 2010 American Physical Society.

block copolymers in water[32] which is a good solvent for the PEO block and a poor solvent for the PB block, Figure 6. Except for the network morphologies, which are not analyzed in our theoretical studies, relative positions of spherical micelles (S and fcc in Figure 6), cylinders (C and $H_1$), lamellae (B and L), inverse cylinders ($H_2$) and inverse spheres (bcc) correspond to the calculated ones. It is worth to be mentioned here that we do not study spatial ordering of the spherical and cylindrical micelles with the increase of the polymer concentration. That is why we relate experimentally detected disordered spherical micelles + fcc structure, cylindrical micelles + hexagonal structure, vesicles + lamellae to spherical, cylindrical, and lamellar structures, respectively.

The $\varphi-\sigma$ phase diagrams are presented in Figure 7. The spherical micelles are always stable in a dilute solution at high fraction of charged groups, $1/\sigma$. In the case of a lower fraction of soluble groups, Figure 7 a, the gradual decrease of the fraction of charged units (increase of $\sigma$) at a fixed polymer concentration first leads to a phase coexistence of the spheres with lamellae (cylinders). Upon further increase of $\sigma$, the system precipitates forming inverse spherical micelles with hollow core. Thus, neutralization of such a system promotes precipitation and one can say that a copolymer with $f = 0.03$ is "tuned" on the formation of inverse micelles. On the contrary, the gradual neutralization of the copolymer with $f = 0.06$ in the dilute regime, Figure 7 b, results in the coexistence of the spheres with lamellae. Taking into account the slope of the boundary of the lamellar phase, one can expect that complete neutralization of the system ($\sigma = \infty$) should result in a stable lamellar phase. The argument supporting this expectation is that the neutral copolymer with $f = 0.06$ always forms lamellae in dilute solution, see simplified diagram, Figure 5. Therefore, we can say that such a copolymer is "tuned" on lamellae. In the concentrated regime, the neutralization of the copolymer does not play an important role and the morphology is primarily controlled by the polymer concentration.

The radius of the micelles (corona) or the semithickness of the lamella, $R_1/a$ (red), is plotted in Figure 8 as a function of the average polymer volume fraction $\varphi$. In contrast to neutral copolymers[6] and to models of charged micelles with the assumption of local neutrality,[8,9,18−20] the size of the spherical micelles increases with $\varphi$ rather than remaining constant. This effect has a

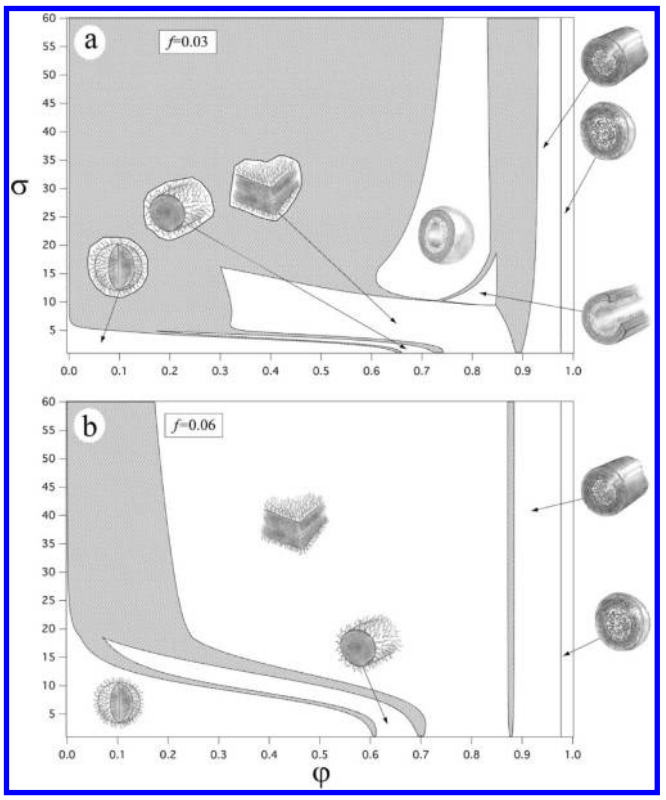


**Figure 7.** $\varphi-\sigma$ phase diagrams of the copolymer at different values of the fraction of soluble units $f$: $f = 0.03$ (a), and 0.06 (b). The shaded areas correspond to the phase coexistence.

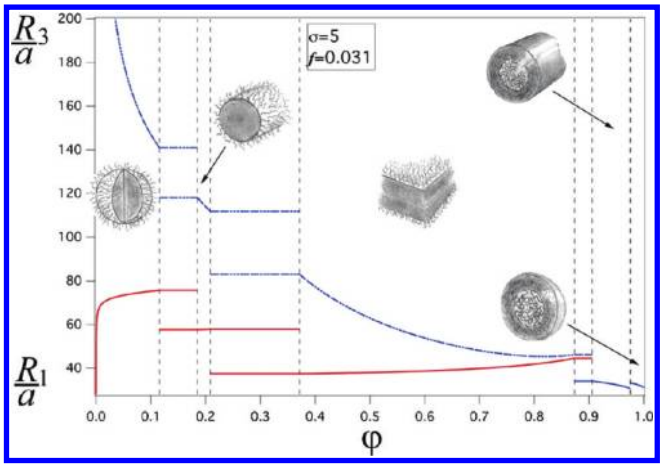


**Figure 8.** Radius of the micelles (semithickness of the lamella), $R_1/a$ (red), and semidistance between the micelles, $R_3/a$ (blue), as functions of the average polymer volume fraction, $\varphi$. Breaks and overlaps of these lines correspond to the phase separation regions. $R_1$ and $R_3$ are constant in these regions. $\sigma = 5$ and $f = 0.031$.

clear physical meaning and is related to the entropy of counterions and electrostatic interactions. The increase of $\varphi$ leads to a decrease of the intermicellar distance, $R_3/a$ (blue) in Figure 8. Therefore, the distribution of counterions between the zones becomes more homogeneous (let us remind that the distribution is fully homogeneous when the coronae are in contact with each other) and the difference in the osmotic pressures of counterions inside and outside the corona diminishes. Also, the electrostatic repulsion between noncompensated charged units in the corona decreases because of the increasing number of counterions inside the corona. All these effects result in the decrease of swelling of the corona-forming blocks. Therefore, to maintain the swelling,

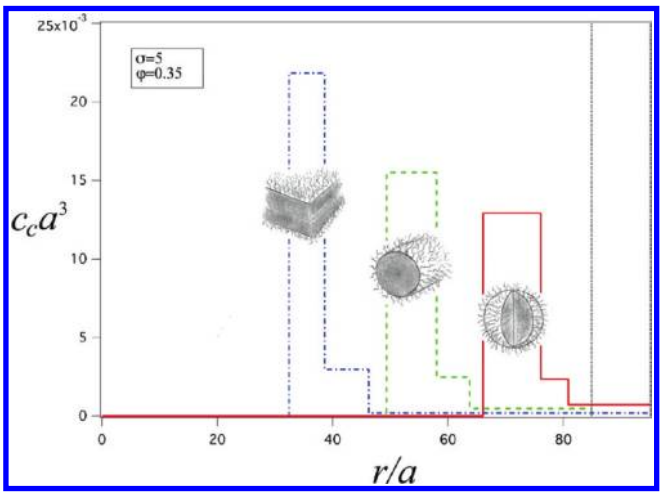


**Figure 9.** Volume fraction of counterions $c_c a^3$ at the distance $r/a$ from the center of lamella (blue, $f = 0.025$), cylindrical micelle (green, $f = 0.035$), and spherical micelle (red, $f = 0.04$). All these distribution functions are calculated at fixed value of polymer concentration, $\varphi = 0.35$. Black vertical dotted lines correspond to the semidistance between the micelles ($R_3/a$).

more molecules aggregate increasing thus the size of the micelle. The thickness of the cylindrical micelles is smaller than the one of the spherical micelles, Figure 8. This effect is primarily controlled by the elasticity of the core-forming blocks and by electrostatic interactions. The elastic free energy of the A block, eq 2, and the electrostatic energy, eq 18, which are proportional to the square of the radius of the core $R_0$, are higher for cylinders. Therefore, to lower these contributions, the radius of the core of the cylinder (and overall thickness) has to be smaller than the radius of the sphere. The same arguments can be applied to explain the difference in the thicknesses of cylinders and lamellae. Comparing $R_1$ and $R_3$, we can conclude that for the particular choice of the parameters in Figure 8 ($\sigma = 5$ and $f = 0.031$) phases with densely packed aggregates are formed only starting from lamellar structure at high $\varphi$ (converging blue and red lines).

The distribution of counterions around the micelles (lamellae) is shown in Figure 9. The space on the left-hand side from each of the functions (where $c_c = 0$) corresponds to the core which is inaccessible for counterions. Maximum, intermediate and minimum values of each function are the concentrations of counterions in the first, second and third zones, respectively. The black vertical dotted lines depict the boundaries of the cells (semidistance between the micelles, $R_3/a$). As one would expect, the maximum concentration of counterions arises in the corona (for all morphologies) to decrease the charge of the soluble blocks. The zone adjoined to the corona (the second zone) has a higher concentration of counterions than the third zone to compensate for the still remaining charge of the corona. If we compare $c_{c1}$ and $c_{c2}$ among different morphologies, one can see that each of them decreases from the lamellae to the spheres, Figure 9. On the contrary, $c_{c3}$ increases. Therefore, the lamellar structure has the minimum fraction of osmotically active[33] counterions (most of them are passive, i.e., condensed), and the spheres have the minimum fraction of the condensed counterions. Such a distribution is the consequence of the electrostatic energy dependence of different morphologies on the volume. The energy of the sphere is finite even in the infinite volume. Therefore, the counterions have a relatively high degree of freedom. The electrostatic energy of an infinite charged plane grows linearly with the distance from it. Therefore, counterions must be condensed to provide a finite value of the energy, i.e., they possess much lower mobility than counterions of the spheres. These results are fully consistent with recent SCFT studies.[25] In the latter paper, an analysis of the

counterion distribution in salt-free solutions of spherical polyelectrolyte brushes and polyelectrolyte stars (brush of high curvature) was performed on the basis of the Poisson−Boltzmann approximation. The authors demonstrated that in both cases a majority of the counterions are localized inside the brush (or star) provided that the grafting density is sufficiently high (the chains are radially stretched like in micelles). Furthermore, in the case of a weakly curved (or planar) brush, a strongly inhomogeneous distribution of "escaped" counterions outside the brush (Gouy−Chapman layer) was observed. In contrast, for polyelectrolyte stars the counterions outside the corona are distributed more uniformly.

In most of the theoretical studies of micelle formation by diblock copolymers, there is no distinctions between lamellae and vesicles (closed bilayer). The latter are experimentally observed at small polymer concentrations. In our approach, the electrostatic contribution to the free energy of the vesicle is essentially different from that of the lamella. In the present paper, we analyze neither the stability of the vesicles nor that of finite-size worm-like micelles whose electrostatic energy is different from that of the infinite cylinders. This will be done in forthcoming publications.

## 6. Conclusions

We have developed a mean-field theory of micelle formation in a salt-free solution of diblock copolymers with a polyelectrolyte block. The so-called *three-zone* model was used which is a simplified alternative of the Poisson−Boltzmann approximation. This model allows to analyze the inhomogeneous distribution of counterions outside the corona (an analogue of Gouy−Chapman layer and Manning condensation). Both dilute and concentrated regimes were analyzed. Phase diagrams including phase coexistence regions were constructed. In addition to conventional "direct" micelles (soluble spheres, cylinders and lamellae), "inverse" cylindrical and spherical structures were predicted to be stable. These predictions are consistent with experimental observations.[32,34] We have shown that the presence of charged groups practically does not change the phase behavior of the solution at high concentration. In this regime, the main factor governing the swelling of the coronae is the polymer concentration. On the other hand, the role of the charged groups at low concentrations is very important. The Rayleigh instability[26] prevents the formation of nonspherical micelles at low polymer concentration. Also the charged groups enhance the stability of the spherical micelles: they are stable, having short enough soluble blocks whereas the neutral micelles precipitate.

**Acknowledgment.** The financial support of the Ministry of Education and Science (Russian Federation), the Deutsche Forschungsgemeinschaft within SFB 569, and the DAAD is gratefully acknowledged.

## References and Notes

(1) Smart, T.; Lomas, H.; Massignani, M.; Flores-Merino, M. V.; Ruiz Perez, L.; Battaglia, G. *Nano Today* **2008**, *3*, 34.
(2) Förster, S.; Abetz, V.; Müller, A. H. E. *Adv. Polym. Sci.* **2004**, *166*, 173.
(3) Zhang, L.; Eisenberg, A. *Science* **1995**, *268*, 1728.
(4) Soo, P. L.; Eisenberg, A. *J. Polym. Sci., Part B* **2004**, *42*, 923.
(5) Halperin, A.; Alexander, S. *Macromolecules* **1989**, *22*, 2403.
(6) Birshtein, T. M.; Zhulina, E. B. *Polymer* **1989**, *30*, 170.
(7) Marko, J. F.; Rabin, Y. *Macromolecules* **1992**, *25*, 1503.
(8) Borisov, O. V.; Zhulina, E. B. *Macromolecules* **2002**, *35*, 4472.
(9) Borisov, O. V.; Zhulina, E. B. *Langmuir* **2005**, *21*, 3229.
(10) Kabanov, A. V.; Kabanov, V. A. *Adv. Drug Delivery Rev.* **1998**, *30*, 49.
(11) Götting, N.; Fritz, H.; Maier, M.; von Stamm, J.; Shoofs, T.; Bayer, E. *Colloid Polym. Sci.* **1999**, *277*, 145.
(12) Perelstein, O. E.; Ivanov, V. A.; Möller, M.; Potemkin, I. I. *Macromolecules* **2010**, *43*, 5442.
(13) Khokhlov, A. R.; Kramarenko, E. Yu. *Macromolecules* **1996**, *29*, 681.
(14) Erel, I.; Zhu, Zh.; Sukhishvili, S.; Patyukova, E.; Potemkin, I.; Kramarenko, E. *Macromol. Rapid Commun.* **2010**, *31*, 490.
(15) Shusharina, N. P.; Nyrkova, I. A.; Khokhlov, A. R. *Macromolecules* **1996**, *29*, 3167.
(16) Shusharina, N. P.; Linse, P.; Khokhlov, A. R. *Macromolecules* **2000**, *33*, 3892.
(17) Oosawa, F. *Polyelectrolytes*; Dekker: New York, 1971.
(18) Netz, R. R. *Europhys. Lett.* **1999**, *47*, 391.
(19) Borisov, O. V.; Zhulina, E. B. *Macromolecules* **2003**, *36*, 10029.
(20) Zhulina, E. B.; Borisov, O. V. *Macromolecules* **2005**, *38*, 6726.
(21) Mochizuki, S.; Komura, S.; Kato, T. *Soft Materials* **2006**, *3*, 89.
(22) Potemkin, I. I.; Andreenko, S. A.; Khokhlov, A. R. *J. Chem. Phys.* **2001**, *115*, 4862.
(23) Limberger, R. E.; Potemkin, I. I.; Khokhlov, A. R. *J. Chem. Phys.* **2003**, *119*, 12023.
(24) Oskolkov, N. N.; Potemkin, I. I. *Macromolecules* **2007**, *40*, 8423.
(25) Leermakers, F. A. M.; Ballauff, M.; Borisov, O. V. *Langmuir* **2008**, *24*, 10026.
(26) Rayleigh, Lord *Philos. Mag.* **1882**, *14*, 184.
(27) Manning, G. S. *J. Chem. Phys.* **1969**, *51*, 924.
(28) Gouy, G. *J. Phys. Theor. Appl.* **1910**, *9*, 457.
(29) Chapman, D. L. *Philos. Mag.* **1913**, *25*, 475.
(30) Semenov, A. N. *Sov. Phys. JETP* **1985**, *61*, 733.
(31) Alexander, S. *J. Phys.* (*Paris*) **1977**, *38*, 983.
(32) Jain, S.; Gong, X.; Scriven, L. E.; Bates, F. S. *Phys. Rev. Lett.* **2006**, *96*, 138304.
(33) Zeldovich, K. B.; Khokhlov, A. R. *Macromolecules* **1999**, *32*, 3488.
(34) Zhang, L.; Bartels, C.; Yu, Y.; Shen, H.; Eisenberg, A. *Phys. Rev. Lett.* **1997**, *79*, 5034.